Journal of Molecular Catalysis A: Chemical 398 (2015) 26–34

Contents lists available at ScienceDirect

Journal of Molecular Catalysis A: Chemical

journal homepage: www.elsevier.com/locate/molcata

Synthesis of octahydro-2*H*-chromen-4-ol from vanillin and isopulegol over acid modified montmorillonite clays: Effect of acidity on the Prins cyclization

Maria N. Timofeeva[a,b,c,*], Konstantin P. Volcho[b,d], Oksana S. Mikhalchenko[b], Valentina N. Panchenko[a,b], Victoria V. Krupskaya[e,f], Sergey V. Tsybulya[a,b], Antonio Gil[g,**], Miguel A. Vicente[h], Nariman F. Salakhutdinov[b,d]

[a] *Boreskov Institute of Catalysis SB RAS, Prospekt Akad. Lavrentieva 5, 630090 Novosibirsk, Russian Federation*
[b] *Novosibirsk State University, Pirogova St. 2, 630090 Novosibirsk, Russian Federation*
[c] *Novosibirsk State Technical University, Prospekt K. Marksa 20, 630092 Novosibirsk, Russian Federation*
[d] *Novosibirsk Institute of Organic Chemistry SB RAS, Prospekt Akad. Lavrentieva 9, 630090 Novosibirsk, Russian Federation*
[e] *Institute of Geology of Ore Deposits, Petrography, Mineralogy and Geochemistry RAS, Staromonetny Pr. 35, 119017 Moscow, Russian Federation*
[f] *Moscow State University, Leninskie Gory 1, 119991 Moscow, Russian Federation*
[g] *Department of Applied Chemistry, Public University of Navarra, 31006 Pamplona, Spain*
[h] *Department of Inorganic Chemistry, University of Salamanca, Salamanca, Spain*

ARTICLE INFO

Article history:
Received 9 October 2014
Received in revised form
15 November 2014
Accepted 17 November 2014
Available online 24 November 2014

Keywords:
Acid-activated montmorillonite
Prins cyclization reaction
Octahydro-2*H*-chromen-4-ol
(−)-Isopulegol
Vanillin

ABSTRACT

Two calcium-rich natural layered aluminosilicates containing 90–95 wt.% montmorillonite were chemically activated using 0.125–3.0 M HCl solutions. Structural and textural properties were characterized by X-ray diffraction, elemental analysis and N_2-adsorption/desorption analyses. According to infrared spectroscopy using pyridine as probe molecule, the amount of Brønsted acid sites increased when increasing HCl concentration. The catalytic performance of these materials was investigated in the Prins cyclization of (−)-isopulegol with vanillin to form octahydro-2*H*-chromen-4-ol, carried out in toluene at 35 °C. It was found that the amount of Brønsted acid sites and the microporosity of the catalysts are key factors for the control of the reaction rate and the selectivity towards octahydro-2*H*-chromen-4-ol.

1. Introduction

The construction of six-membered oxygen-containing heterocycles with tetrahydropyran moiety is widely used for the synthesis of several biologically active compounds having analgesic, anti-inflammatory, antiproliferative and cytotoxic activity [1–4]. Reaction of homoallylic alcohols with aldehydes, variant of the Prins cyclization reaction, is one of the ways for the synthesis of a wide range of tetrahydropyran derivatives [1,4]. Both Brønsted [5–7] and Lewis acids [7–9] can catalyze Prins cyclization reaction of (−)-isopulegol with aldehydes containing electron-donating and electron-withdrawing substituents, allowing to obtain a variety of octahydro-2*H*-chromen-4-ols. Thus, the synthesis of octahydro-2*H*-chromen-4-ols from (R)-citronellal and aldehydes using $Sc(OTf)_3$ as catalyst was demonstrated by Yadav et al. [8]. Silva and Quintiliano [10] reported the Prins cyclization of (−)-isopulegol with *p*-anisaldehyde in the presence of molecular iodine as a homogeneous catalyst. Octahydro-2*H*-chromen-4-ols with good yields have been synthesized from (−)-isopulegol and various types of aldehydes in the presence of acid-activated montmorillonites K10 [4] and KSF [8].

Recently, acid-activated montmorillonites have received much attention in organic synthesis due to their unique structural and physicochemical properties, their wide potential applicability and low cost. The lamellar structure of montmorillonite (MM) consists of the negative charged parallel layers of two tetrahedral silicate and one octahedral aluminate sheets, with charge compensating

* Corresponding author at: Boreskov Institute of Catalysis SB RAS, Prospekt Akad. Lavrentieva 5, 630090 Novosibirsk, Russian Federation. Tel.: +7 383 330 7284; fax: +7 383 330 8056.
** Corresponding author at: Department of Applied Chemistry, Los Acebos Building, Public University of Navarra, Campus of Arrosadia s/n, 31006 Pamplona, Spain. Tel.: +34 948 169602; fax: +34 948 169602.
E-mail addresses: timofeeva@catalysis.ru (M.N. Timofeeva), andoni@unavarra.es (A. Gil).

http://dx.doi.org/10.1016/j.molcata.2014.11.016
1381-1169/

cations located between these layers. The interlayer cations can be exchanged and, therefore, chemical and catalytic properties of the clay can be adjusted. It is well known that acid activation of clays generates Brønsted acid sites, which are important for carrying out organic transformations. Because of the appearance of strong Brønsted acid sites, acid-activated clays are widely used for isomerization [11], alkylation [12,13] and acylation [14] reactions. Note that the variation of the strength and the number of acid sites allows adjusting the activity of acid-activated clays; therefore the tailored design of acid-activated clays is crucial for the application of the resulting catalysts in particular reactions.

In this work, we investigate the catalytic performance of two series of acid-activated clays in the Prins cyclization reaction (Reaction 1) of (−)-isopulegol (**I**) with vanillin (**II**) to octahydro-2*H*-chromen-4-ol (isomers **IIIa** and **IIIb**). The clays are two calcium-rich natural layered aluminosilicates (90–95 wt.% montmorillonite) from beds located in Mukhortala (Buryatia, Russia, denoted as MM^R) and Tagansk (Kazakhstan, denoted as MM^K).

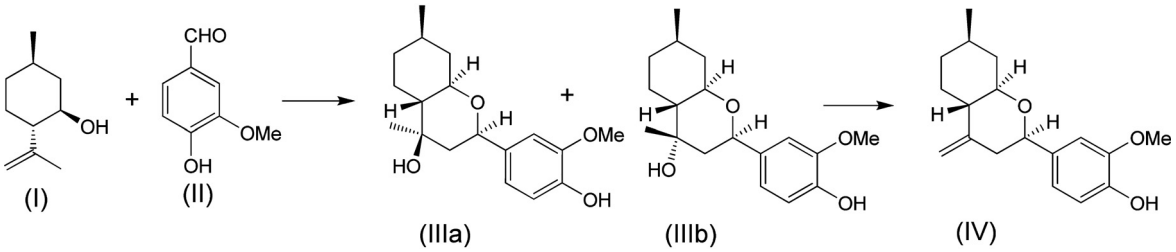

(R.1)

One of the tasks of our study was to reveal the effect of the HCl concentration used for the acid-activation on the surface acidity and the porous structure of the aluminosilicates, and the subsequent influence on the catalytic activity of these solids. It is well known that the chemical composition and textural properties of the original clays influence the surface acidity and the porous structure of their acid-activated derivatives. Therefore, the next aim of our study was to investigate the effect of the nature of the original clays on these parameters. IR spectroscopy using pyridine as probe molecule was used for the analysis of surface acidity of the acid-activated clays. A priori, the amount of the Brønsted acid sites, adjusted by the HCl concentration, may allow to control the surface acidity and the porous structure of the acid-activated MMs and also their catalytic performance in the Prins cyclization reaction of (−)-isopulegol with vanillin to octahydro-2*H*-chromen-4-ol in toluene.

2. Experimental

2.1. Materials

(−)-Isopulegol and vanillin were purchased from Acros Organic. The natural clays were two calcium-rich natural layered aluminosilicates (90–95 wt.% montmorillonite) from beds located in Mukhortala (Buryatia, Russia) and Tagansk (Kazakhstan). Chemical composition of these clays is shown in Table 1.

2.2. Modification of the montmorillonites by HCl

5 g of MM^R or MM^K were suspended in 150 cm^3 of aqueous solutions of 0.125–3.0 M of HCl and the mixture was stirred at room temperature for 7 days. Then, the solid was separated, washed with water and dried at room temperature. The designation of the samples and the conditions of their synthesis are presented in Table 1.

2.3. Instrumental measurements

The porous structure of the materials was studied from nitrogen (Air Liquide, 99.999%) adsorption at −196 °C using a static volumetric apparatus (Micromeritics ASAP 2010 adsorption analyser). All samples (0.2 g) were degassed for 24 h at 200 °C at a pressure lower than 0.133 Pa. The specific surface area (S_{BET}) was calculated from the adsorption data over the relative pressure range between 0.05 and 0.20. The total pore volume (V_Σ) was calculated from the amount of nitrogen adsorbed at a relative pressure of 0.99. The micropore volume ($V\mu$) and the external specific surface area (S_{ext}) were calculated using the *t*-plot method, and the pore diameter applying the BJH method.

The chemical analyses of the solids were carried out by means of inductively coupled plasma-atomic emission spectrometry (ICP-AES).

The X-ray diffraction patterns from random samples were collected on a X-ray diffractometer (Ultima-IV, Rigaku) with Cu-K_α radiation (λ = 1.54056 Å), rapid detector D/Tex, scan range 3.6–65° 2θ, scan speed 5°/min, step 0.02° 2θ, maximum intensity ~25,000 counts. The values of coherent scattering area by the (0 0 1) direction are estimated by Scherrer formula (Eq. (1)):

$$h = K \cdot \frac{\lambda}{\beta} \cdot \cos(\theta) \quad (1)$$

where h is the mean size of the ordered (crystalline) domains, which may be smaller or equal to the grain size; K is a dimensionless shape factor, with a value close to unity. The shape factor has a typical value of about 0.9, but varies with the actual shape of the crystallite; λ is the X-ray wavelength, β is the line broadening at half of the maximum intensity (FWHM), after subtracting the instrumental line broadening, denoted as $\Delta(2\theta)$; and θ is the Bragg angle.

2.4. Infrared spectroscopy measurements

For studies of Brønsted surface acidity, the samples were pressed into self-supporting wafers (10–25 mg/cm^2) and pretreated within the IR cell by heating at 500 °C in air for 1h and then under vacuum for 1 h before the adsorption experiments. Then, the samples were exposed to saturated pyridine vapours at room temperature for 10 min and for 15 min at 150 °C. Then pyridine was desorbed at 150 °C until a pressure of 10^{-6} mbar, when there is no more physisorbed pyridine on the wafers. The strength of Brønsted acid sites was characterized by the *PA* values calculated using Eq. (2) [15]:

$$PA = \frac{\log(3400 - \nu_{NH})}{0.0023} - 51 \quad (2)$$

where *PA* (kJ/mol) is the energy of proton elimination from the acid residue, 3400 cm^{-1} is the wavenumber of the band of the undisturbed N—H bond of the pyridinium ion, and ν_{NH} (cm^{-1}) is

Table 1
Chemical composition of natural and acid-activated montmorillonites.

	Experimental conditions		Chemical composition (wt.%)						Si/Al (mol/mol)
	HCl (mol/dm^3)	HCl/clay (mmol/g)	Si	Al	Na	Fe	Mg	Ca	
MM^R	–	–	28.5	7.2	0.1	0.8	0.8	1.1	4.0
0.25 M MM^R	0.25	7.5	31.6	7.4	0.1	0.8	0.7	0.3	4.4
0.5 M MM^R	0.50	15.0	33.2	8.1	0.1	0.7	0.5	Trace	4.2
1.0 M MM^R	1.0	30.0	36.3	6.9	0.1	0.7	0.4	Trace	5.4
3.0 M MM^R	3.0	90.0	33.1	3.3	0.03	0.7	0.1	Trace	10.8
MM^K	–	–	24.1	10.7	0.1	0.6	2.4	1.5	2.34
0.125 M MM^K	0.125	3.75	23.3	11.7	0.2	0.6	2.0	0.3	2.07
0.25 M MM^K	0.25	7.5	25.4	12.4	0.1	0.5	1.7	Trace	2.12
0.50 M MM^K	0.50	15.0	27.5	12.9	0.2	0.5	1.3	Trace	2.12

the wavenumber of the centre of gravity of the band of the stretching vibration of the pyridinium ion, which depends on the basicity of the acid residue and is determined from the contour of the ν_{NH} band.

The amount of Brønsted acid sites was estimated from the intensity of the band of the stretching vibration of pyridinium ions with a maximum at 1540 cm^{-1} using Eq. (3):

$$A = 10^{-3} \cdot A_0 \cdot C_s \cdot \rho \quad (3)$$

where A is the integral intensity of the band (cm^{-1}); A_0 is the integral intensity of the band at 1 μmol of pyridine adsorbed on 1 g of sample; C_s is the amount of pyridine adsorbed on sample; ρ is the thickness of the tablet (mg/cm^2) ($A_0^{1545-1548\,cm^{-1}} = 3$ cm^2/mmol) [15]. IR spectra were recorded on a Shimadzu FTIR-8300S spectrometer in the range between 400 and 6000 cm^{-1} with a resolution of 4 cm^{-1}.

2.5. Catalytic tests

The reaction of vanillin with (−)-isopulegol was carried out at 35 °C in a glass vial (15 cm^3) equipped with a magnetic stirrer. Before the reaction, all materials were treated at 150 °C for 2 h to remove residual water in the samples. The standard procedure was as follows: 0.65 mmol of vanillin in 4 cm^3 of toluene was added to 100 mg of catalyst and 48 mg (0.26 mmol) of tridecane. Then, 0.65 mmol of (−)-isopulegol were introduced into the reactor. At various time intervals, aliquots were taken from the reaction mixture and analyzed after separation by centrifugation of the catalysts. The products were analyzed using a gas chromatograph (Agilent 7820) with a flame ionization detector on a capillary column (HP-5). Tridecane was used as the internal standard.

Compounds (**IIIa**–**b**) and (**IV**) were isolated using column chromatography. Their structure was confirmed by NMR (Bruker AV-400, $CDCl_3$) and HR-MS (DFS-Thermo-Scientific spectrometer).

2.5.1. Compound (***IIIa***)

^{1}H NMR: 0.94–1.08 (m, 1H, H_a-8); 0.91 (d, $J_{18,9}$ =6.6 Hz, 3H, H-18); 0.94–1.08 (m, 1H, H_a-7); 1.09 (d, $J_{10a,10e}$ = 12.3 Hz, $J_{10a,1a}$ = 10.8 Hz, 1H, H_a-10); 1.26 (s, 3H, H-17); 1.27 (ddd, $J_{6a,7a}$ = 12.2 Hz, $J_{6a,1a}$ = 10.2 Hz, $J_{6a,7e}$ = 3.3 Hz, 1H, H_a-6); 1.37–1.52 (m, 1H, H_a-9); 1.56 (br. s, 1H, OH); 1.66–1.81 (m, 2H, He-8, H_a-4); 1.92 (dddd, $J_{7e,7a}$ = 12.8 Hz, $J_{7e,6}$ = $J_{7e,8a}$ = $J_{7e,8e}$ = 3.3 Hz, 1H, H_e-7); 1.99 (dm, $J_{10e,10a}$ = 12.3 Hz, 1H, H_e-10); 3.23 (ddd, $J_{1a,10a}$ = 10.8 Hz, $J_{1a,6a}$ = 10.2 Hz, $J_{1a,10e}$ = 4.3 Hz, 1H, H_a-1); 3.86 (s, 3H, OMe); 4.34 (dd, $J_{3a,4a}$ = 11.7 Hz, $J_{3a,4e}$ = 2.2 Hz, 1H, H_a-3); 6.79 (d, $J_{15,16}$ = 1.8 Hz, 1H, H-15); 6.81 (s, 1H, H-12); 6.86 (d, $J_{16,15}$ = 1.8 Hz, 1H, H-16). ^{13}C NMR: 76.59 (d, C-1); 74.56 (d, C-3); 49.95 (t, C-4); 70.89 (s, C-5); 51.91 (d, C-6); 22.96 (t, C-7); 34.28 (t, C-8); 31.36 (d, C-9); 41.42 (t, C-10); 134.12 (s, C-11); 108.61 (d, C-12); 144.93 (s, C-13); 146.36 (s, C-14); 119.05 (d, C-15); 113.95 (d, C-16); 21.26 (q, C-17); 22.10 (q, C-18); 55.75 (q, C-19). HR-MS: 306.1829 (M^+, $(C_{18}H_{26}O_4)^+$; calc. 306.1826).

2.5.2. Compound (***IIIb***)

We identified characteristic signal at 4.69 ppm (dd, $J_{3a,4a}$ = 11.5 Hz, $J_{3a,4e}$ = 2.2 Hz, 1H, H_a-3) in ^{1}H NMR only due to overlapping of signals with the corresponding signals of the major isomer (**IIIa**). ^{13}C NMR: 76.59 (d, C-1); 75.53 (d, C-3); 48.00 (t, C-4); 69.49 (s, C-5); 49.31 (d, C-6); 22.45 (t, C-7); 34.28 (t, C-8); 31.19 (d, C-9); 41.42 (t, C-10); 134.76 (s, C-11); 108.71 (d, C-12); 144.93 (s, C-13); 146.36 (s, C-14); 118.88 (d, C-15); 113.95 (d, C-16); 20.93 (q, C-17); 22.10 (q, C-18); 55.75 (q, C-19).

2.5.3. Compound (***IV***)

^{1}H NMR: 0.95 (d, $J_{18,9a}$ =6.6 Hz, 3H, H-18); 1.00 (dm, $J_{8a,8e}$ = 12.8 Hz, 1H, H_a-8); 1.09 (ddd, $J_{10a,10e}$ = $J_{10a,9a}$ = 12.2 Hz, $J_{10a,1a}$ = 11.0 Hz, 1H, H_a-10); 1.15–1.28 (m, 1H, H_a-7); 1.42–1.55 (m, 1H, H_a-9); 1.74 (dddd, $J_{8e,8a}$ = 13.0 Hz, $J_{8e,7a}$ = 3.7 Hz, $J_{8e,7e}$ = 3.3 Hz, $J_{8e,10e}$ = 2.0 Hz, 1H, H_e-8); 1.81–1.84 (m, 1H, H_a-6); 1.89 (dddd, $J_{7e,7a}$ = 13.0 Hz, $J_{7e,6a}$ = $J_{7e,8a}$ = 3.7 Hz, $J_{7e,8e}$ = 3.3 Hz, 1H, H_e-7); 1.99 (dddd, $J_{10e,10a}$ = 12.2 Hz, $J_{10e,1a}$ = $J_{10e,9a}$ = 4.1 Hz, $J_{10e,8e}$ = 2.0 Hz, 1H, H_e-10); 2.35 (ddm, $J_{4a,4e}$ = 13.1 Hz, $J_{4a,3a}$ = 11.4 Hz, 1H, H_a-4); 2.45 (dd, $J_{4e,4a}$ = 13.1 Hz, $J_{4e,3a}$ = 2.6 Hz, 1H, H_e-4); 3.10 (ddd, $J_{1a,10a}$ = 11.0 Hz, $J_{1a,6a}$ = 9.8 Hz, $J_{1a,10e}$ = 4.1 Hz, 1H, H_a-1); 3.85 (s, 3H, OMe); 4.31 (dd, $J_{3a,4a}$ = 11.4 Hz, $J_{3a,4e}$ = 2.6 Hz, 1H, H_a-3); 4.66, 4.78 (2m, all $J \leq 2.2$ Hz, 2H, H-17); 5.81 (s, 1H, H-12); 6.83 (d, $J_{15,16}$ = 1.8 Hz, 1H, H-15); 6.91 (d, $J_{16,15}$ = 1.8 Hz, 1H, H-16). ^{13}C NMR: 81.85 (d, C-1); 76.29 (d, C-3); 44.35 (t, C-4); 146.31 (s, C-5); 46.32 (d, C-6); 25.98 (t, C-7); 34.04 (t, C-8); 31.35 (d, C-9); 41.38 (t, C-10); 134.42 (s, C-11); 108.55 (d, C-12); 144.87 (s, C-13); 148.28 (s, C-14); 113.93 (d, C-15); 118.92 (d, C-16); 105.45 (q, C-17); 22.15 (q, C-18); 55.74 (q, C-19). HR-MS: 288.1723 (M^+, $(C_{18}H_{24}O_3)^+$; calc. 288.1720).

3. Results and discussion

3.1. Structural properties of HCl-activated montmorillonite catalysts

The chemical composition of the acid-activated MMs is shown in Table 1. As can be observed, the composition of the MMs varies when increasing the HCl concentration in the course of the acid treatments. The effect of HCl concentration on chemical composition of MM can be divided in two regions. When HCl concentration was less than 0.5 M, the Si/Al molar ratio remained constant; the elimination of the exchangeable Ca^{2+} cations seems to be the only effect on the composition of the solids. Indeed, the leaching of Ca^{2+} cations from MM^R and MM^K by 0.5 M HCl was 95.7% and 97.8%, respectively. However, the changes of the molar ratio Si/Al were significant when HCl concentration was higher than 0.5 M; the higher acid concentration makes that Al^{3+} cations from the octahedral sheet begin to dissolve, while the SiO_2 content does not change because of its insolubility in acid medium, Si/Al ratio thus increasing. It is remarkable that the Si/Al variation is different for both series MM^R and MM^K, and the same happens

Table 2
Textural properties of natural and acid-activated montmorillonites.

	S_{BET} (m^2/g)	S_{ext} (m^2/g)	S_{ext}/S_{BET} (%)	V_{Σ} (cm^3/g)	V_{μ} (cm^3/g)	V_{μ}/V_{Σ} (%)	d_{pore} (nm)
MM^R	105	97	92.4	0.224	0.003	1.3	9.0
0.125 M MM^R	97	89	91.7	0.203	0.003	1.5	7.4
0.25 M MM^R	106	92	86.8	0.232	0.006	2.6	9.0
0.50 M MM^R	111	95	85.6	0.271	0.006	2.2	7.4
MM^K	77	32	41.6	0.104	0.022	21.2	24.0
0.125 M MM^K	69	28	40.6	0.089	0.020	22.5	24.2
0.25 M MM^K	73	26	35.6	0.085	0.022	25.9	24.1
0.50 M MM^K	70	24	34.3	0.077	0.022	28.6	24.1

Table 3
XRD data of natural and acid-activated montmorillonites.

	d_{001} [a] (Å)	h_{001} [b] (nm)	I_{001}/I_{020} [c]
MM^R	15.3	13.8	2.97
0.25 M MM^R	15.4	14.8	3.11
0.50 M MM^R	15.1	7.9	1.57
1.0 M MM^R	13.9	5.6	1.23
3.0 M MM^R	13.1	6.8	1.03
MM^K	13.9	5	0.87
0.125M MM^K	15.4	7.7	1.71
0.25M MM^K	15.4	7.7	1.72
0.50M MM^K	15.5	6.4	1.51

[a] d_{001} – interlayer distance.
[b] $h_{(001)}$ – area of coherent scattering (Eq. (1)).
[c] I_{001}/I_{020} – index of ordering-disordering.

for the textural properties (Table 2). The content of Mg in MM^K clay (2.4%) is clearly higher than in MM^R solid (0.8%), and MM^K has also a higher Ca content (1.5% vs. 1.1%). Thus, the activation of MM^K begins with the exchange of Ca^{2+} cations, and continues with the progressive dissolution of octahedral Mg^{2+}, but without affecting Al^{3+}, whose content even shows a small relative increase (it may be considered that octahedral Mg^{2+} is much more soluble than Al^{3+}). Higher HCl concentrations should be needed to dissolve octahedral Al^{3+} in this clay.

The changes occurring in the course of acid activation can also be detected by X-ray diffractometry. The X-ray diffraction patterns of the samples are shown in Fig. 1. According to the XRD data, MM^R includes microcrystalline opal CT/A as interstitial impurity, as indicated by the diffraction peaks at 4.07, 2.49, 1.87, 1.61 Å and some other reflections with very low intensity [16]. A small amount of quartz (d = 3.34 Å) is observed in MM^K.

It is well known that the structural and textural changes of montmorillonites in the course of any modification can be revealed out by the changes of coherent scattering area and the ratio of I_{001}/I_{020} reflection intensities, which can characterize the crystallites thickness and order-disorder and/or variation of the turbostatic stacking, respectively. The experimental data (Fig. 1, Table 3) point out that the concentration of HCl affects the XRD patterns of acid-modified MMs, i.e. the position, asymmetry and intensity of (0 0 1) reflection. Thus, the modification of MM^K by 0.125 and 0.25 M HCl led to a more intense and more symmetrical (0 0 1) reflection, thus increasing the I_{001}/I_{020} ratio. This phenomenon is likely the result of the equalization of the heights of montmorillonite unit structure, the relative increasing of interlayer ordering and crystallite size, also favoured by the "cleaning" of the solid by the elimination of soluble impurities. At the same time, the crystallite size and the ordering of layers decreased after modification of MM^K by 0.5 M HCl, which can indicate the beginning of montmorillonite dissolution. A similar trend of the structural changes was observed for MM^R series. Note that a gradual and regular decrease in the interlayer space (d_{001}), a broadening of the (0 0 1) reflection (connected to the crystalline thickness) and a decrease of the relative degree of ordering are more predictable for acid-activated MM^R in comparison to MM^K. Effect of HCl concentration on structure of MM samples is in agreement with the evolution of the textural properties.

The specific surface areas (S_{BET}) of the acid-activated MMs have been calculated from nitrogen adsorption isotherms by using the BET method. Table 2 shows the effect of acid treatment on the textural characteristics of MMs. The pore diameter and the S_{BET} for MM^R and MM^K are 9.0 and 24.0 nm, and 105 and 77 m^2/g, respectively. Increasing the HCl concentration does not significantly change the S_{BET} of MMs that remains practically constant, in contrast with the external surface area (S_{ext}) and microporosity. The ratios of S_{ext}/S_{BET} and V_{μ}/V_{Σ} rises with increasing HCl concentration, i.e. acid activation of MMs leads to an increase in microporosity, that can point out the change in the crystallite size and the character of their interaction. Noteworthy, the changes of the microporosity of MM^R series are greater than for MM^K (Table 2). Thus, it may be concluded that the modification of MM by low-concentration HCl leads to a relative increase in the degree of order, crystallite size, S_{BET} and S_{ext}. The dissolving of structure begins at higher HCl concentrations, that is very likely associated with the removal of octahedral cations, that leads to a reduction of the crystallites size and S_{ext} and to an increase of microporosity, as has been previously reported [17].

3.2. IR spectroscopic study of Na-MM materials activated by HCl

IR spectroscopy is a simple and useful technique for the investigation of mineralogical and chemical structure of clay minerals [18,19]. Here, this technique is used for the study of the effect of HCl concentration on the formation of BAS and the structural changes occurring in MM samples during their acid activation.

IR spectra of MM^R, MM^K and their acid-activated samples in the 500–2000 cm^{-1} region are shown in Fig. 2. The intense bands are attributed to ν_s(O—Si—O) (842 cm^{-1}), δ(Si—O) (628 cm^{-1}), the stretching vibrations of silica-oxygen tetrahedra ν_{as}(Si—O—Si(Al)) (1034–1038 cm^{-1}) and a deformation vibration of Al_2OH (917–926 cm^{-1}) [19]. Note that the strong band at 793 cm^{-1} observed in the spectrum of MM^R points out the existence of platy form of disordered tridymite, in agreement with XRD data, or of amorphous silica (usually denoted as free silica).

Moreover, the bands at 841–845 cm^{-1} (AlMgOH) and 882 cm^{-1} (AlFeOH) are observed in the IR spectra of MM samples. The intensities of these bands can be used for the comparison of the amount of Mg and Fe in the solids. The amount of Mg in MM^K is larger in comparison with that in MM^R, while the amount of Fe is larger in MM^R. According to the chemical analysis, the mass contents of Mg and Fe in MM^R and MM^K are 0.8 and 2.4 wt.%, and 0.8 and 0.6 wt.%, respectively. The activation of MM^R and MM^K samples by HCl leads to the change of their chemical composition. It can be seen from IR spectra that the increase in the HCl concentration provokes the reduction in the intensity of the bands at 841–845 and 882 cm^{-1}, that can indicate the leaching of Mg^{2+} and Fe^{3+} cations. The leaching of Mg^{2+} cations from MM^R and MM^K was 85.7% and 45.8%, respectively. At the same time, leaching of Fe^{3+} cations from MM^R and MM^K was 12.5% and 16.7%, respectively. According to IR spectroscopic and

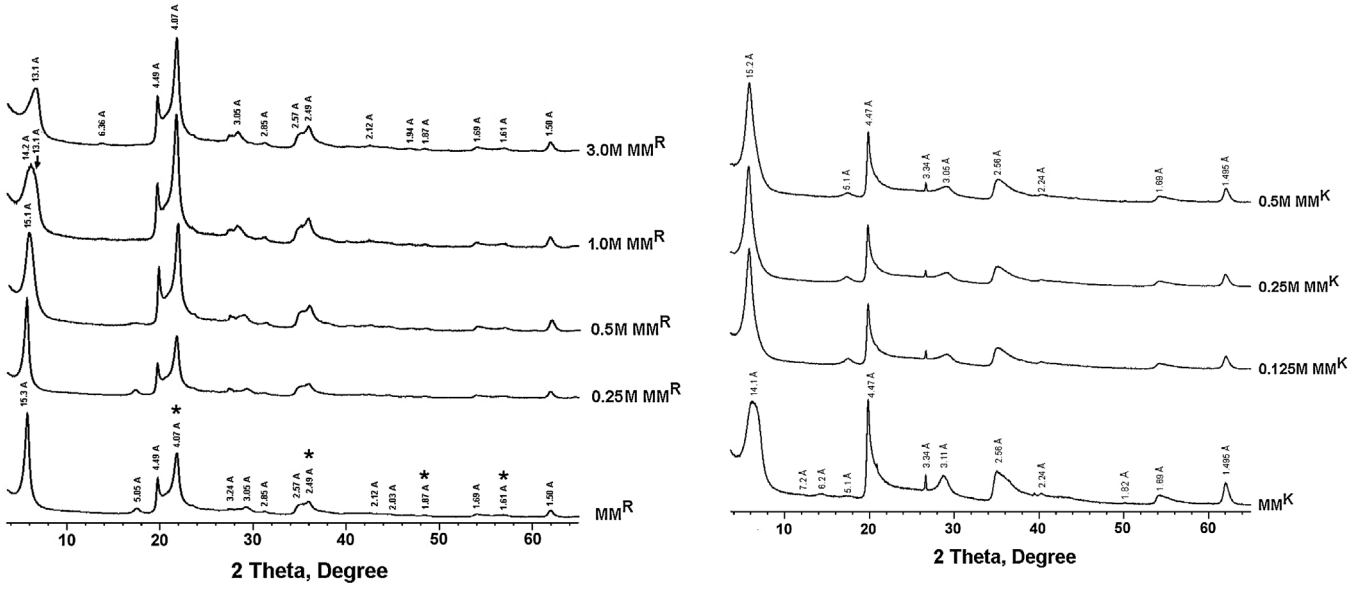

Fig. 1. XRD patterns of natural and acid-activated montmorillonites in MM^R and MM^K series.

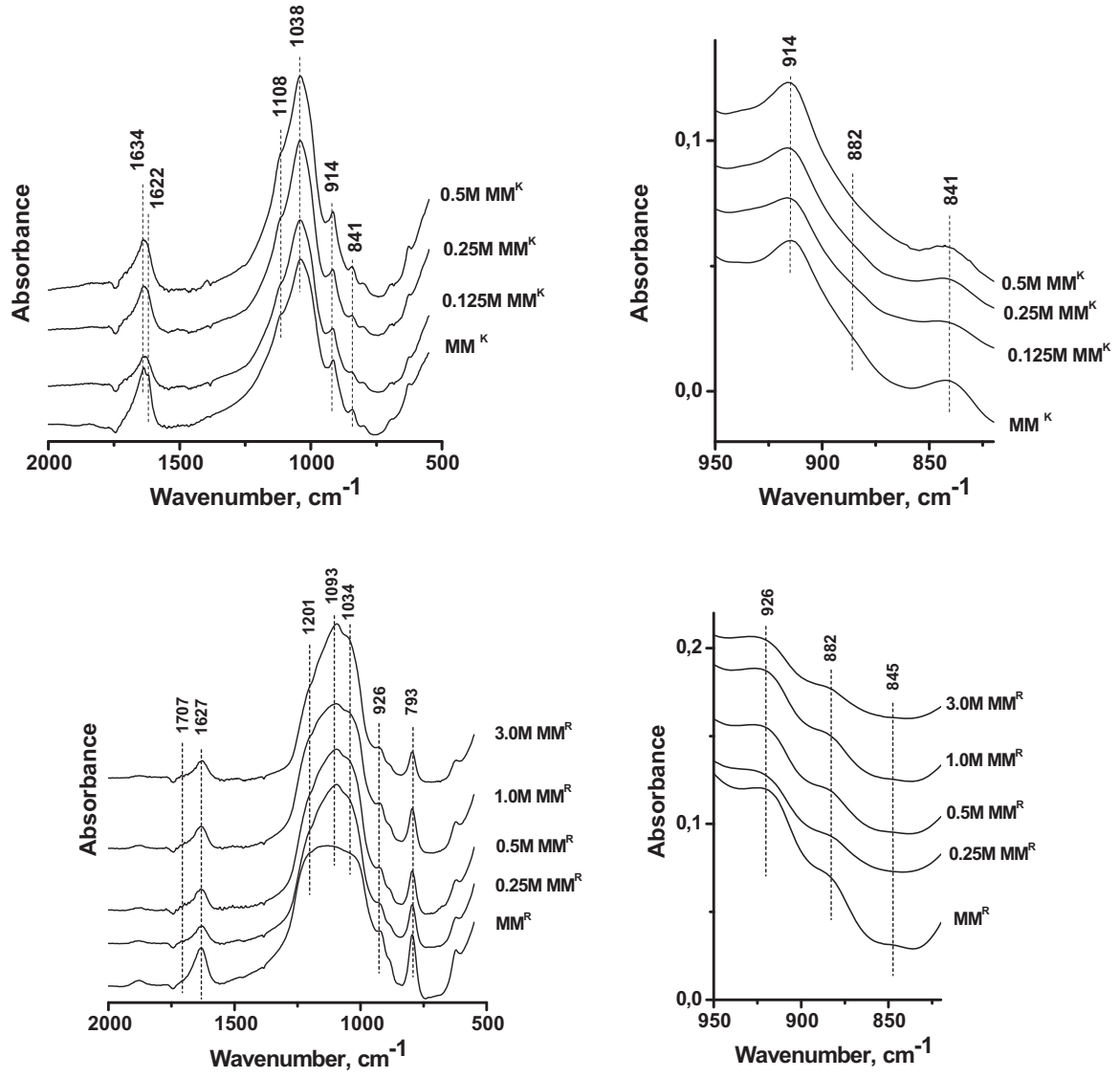

Fig. 2. IR spectra of natural and acid-activated montmorillonites in MM^R and MM^K series.

analytical data, leaching of Mg^{2+} cations is larger in comparison to Fe^{3+} cations in the course of the acid-activation by HCl.

The change of the chemical composition of MM^R can also be confirmed by the shape of the broad band in the region of 950–1250 cm^{-1}, related to the Si—O—Si(Al) bonds, and the decrease in the intensity of the band at 793 cm^{-1}, assigned to opal CT/A or free silica. As can be seen from Table 1, Si/Al molar ratio sharply increases only after the treatment with 1.0 M HCl. It is well known that the tetrahedral layer is more stable towards low acid concentration in comparison to octahedral layer [20,21]. Therefore, the relative increase in Si content in MM samples is caused by the leaching of the exchangeable and octahedral cations.

The change of the surface acidity of MM samples in the course of the acid-activation was investigated by FT-IR spectroscopy using pyridine as probe molecule (Table 4). Experimental data clearly show that the strength of the acid sites (PA) weakly depends on the HCl concentration. The value of *PA* obtained from Eq. (1) for all acid-activated MMs is 1161–1164 kJ/mol. The amount of the Brønsted acid sites of MMs samples rises with increasing HCl concentration up to 1.0 M, i.e. the higher HCl concentration, the larger amount of Brønsted acid sites. As the acid-activation of MM favours the increase in the Si/Al ratio in the region of 4.0–5.4, this suggests that leaching of Al should provoke the increase in the amount of Si—(OH). . .Al groups formed in the tetrahedral layer of the clay. At the same time, the following increasing HCl concentration (>1.0 M) does not lead to the increasing of the amount of BAS; the amounts of BAS for 1.0 M MM^R and 3.0 M MM^R are close. This phenomenon is related to the sharply increasing of Si/Al molar ratio from 5.4 to 10.8. Effect of Si/Al molar ratio on the amount of BAS was investigated for SAPO materials [22]. It was found that the increasing of Si content in the solids favours the formation of Si islands. The numbers of acid sites, i.e. the amount of Si—(OH). . .Al groups, depended on the dimension of the Si islands, which was related to the Si concentration and to the structure topology. We can assume that the sharply increasing of Si/Al molar ratio leads to the formation of the dimension of the Si islands and, therefore, the decreasing amount of Si—(OH). . .Al groups, i.e. amount of BAS.

3.3. Catalytic properties of Na-MM materials modified by HCl

The catalytic properties of the acid-modified clays calcinated at 150 °C were investigated in the Prins cyclization reaction (Reaction 1) of (−)-isopulegol (**I**) with vanillin (**II**) to octahydro-2*H*-chromen-4-ol (isomers **IIIa** and **IIIb**) at 35 °C and a molar ratio of (**I**)/(**II**) 1.0/1.0. MM^R and MM^K were inactive in this reaction. In the presence of acid-activated MM^R and MM^K samples the main products were isomers (**IIIa–b**). Moreover, the product (**IV**) was also formed due to the dehydration of (**III**). The typical kinetic profiles are shown in Fig. 3. According to the experimental data (Fig. 4), the concentration of HCl used for the acid activation of the samples strongly affects the conversion of (**II**), the yield of isomers (**IIIa–b**) and the molar ratio of (**IV**)/(**III**) (Table 4). The conversion of (**II**) increases with increasing the HCl concentration up to 1.0 M, and then does not change. At the same time, the increase in the HCl concentration favours the decrease in the yield of (**III**) and the molar ratio of (**III**)/(**IV**). The maximum yields of (**IIIa–b**) were 75.7 and 71.4% after 2 h of reaction in the presence of 0.125 M MM^R and 0.125 M MM^K solids, respectively.

Analysis of the kinetic profiles (Fig. 3) points out that reaction proceeds with a second-order reaction rate (Eq. (4)):

$$W = k \cdot C_a \cdot C_b \tag{4}$$

where k is the observed kinetic reaction rate, C_a and C_b are the concentrations of (**I**) and (**II**), respectively. As the initial concentration

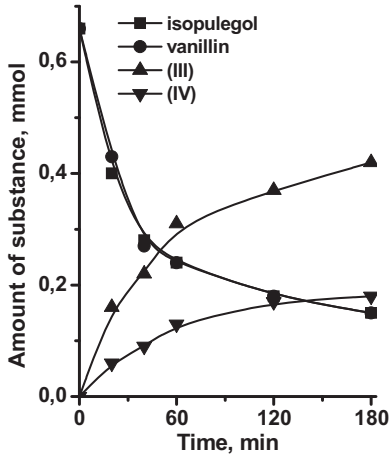

Fig. 3. Evolution of the amount of reactants and products with time of reaction, in the reaction of vanillin with (−)-isopulegol using 0.5 M MM^R catalyst (reaction conditions: 100 mg catalyst, 0.65 mmol (**I**), 0.65 mmol (**II**) in toluene 4 mL, 35 °C).

of (**I**) and (**II**) is the same, the second-order rate constants, k, were calculated from the linear correlations using Eq. (5) (Fig. 5):

$$\frac{1}{(a-x)} = kt + \frac{1}{a} \tag{5}$$

The values of the kinetic constant, k, are shown in Table 4. Experimental data point that the reaction rate depends on the temperature of activation of samples. Thus, values of k for 0.25 M MM^R activated at 150 and 200 °C were 41.2×10^3 and 46.2×10^3 L/mol min, respectively (Table 4). Probably, the small difference of these values can be explained by the effect of the temperature of activation both on the dehydration of the clay and stability of its layer structure. According to Vlasova et al. [23], the increase in the temperature of treatment of bentonite modified by acid leads to the decrease in the interlayer distance (d_{001}). Thus, values of d_{001} are 15.2, 12.5 and 10.9 Å at 25, 150 and 300 °C. Therefore, we can assume that simultaneous dehydration of sample and decreasing of the interlayer space do not favour the considerable increase in the reaction rate. Moreover, it is well known [24] that temperatures of dehydration for sodium- and calcium-rich montmorillonites are 150 and 200 °C, respectively. Therefore, we can assume that the interlayer distance is accessible for exchange processes in the region of calcination temperature of 150–200 °C.

According to these data, catalytic activity, k, rises with the increasing of HCl concentration, which may be related to the variation in the surface acidities. As can be seen from Fig. 6, catalytic activity, k, linearly depends on the amount of Brønsted acid sites, the catalytic activity increases with the amount of Brønsted acid sites. It is noticeable that catalytic activity of 1.0 M MM^R and 3.0 M MM^R are close, because the amount of BAS in both solids is the same (Table 1).

It is of interest to consider the rate constant based on the specific surface area (k_S), which depends on the textural properties and the amount of accessible proton sites. The values of k_S are shown in Table 4. The nature of the clay also affects the correlation between k_S and the amount of BAS. Thus, k_S negligibly increases for acid-activated MM^R solids with increasing the amount of BAS from 5.4 to 14.8 μmol/g. At the same time, for acid-activated MM^K samples the increase in the amount of BAS from 2.3 to 14.7 μmol/g leads to nearly twice rising of k_S (Table 4). These trends are in agreement with the variation of S_{ext} (Table 2), which is important for the reaction mechanism. After acidic modification of MM^R by 0.5 M HCl the value of S_{ext} changes from 97 to 95 m^2/g (~2%), while for MM^K this value changes from 32 to 24 m^2/g (25%). These data indicate that

Table 4
Acidic and catalytic properties of acid-activated montmorillonite catalysts.

	BAS[a] (μmol/g)	PA[b] (kJ/mol)	(**III**)/(**IV**) (mol/mol)	(**IIIa**)/(**IIIb**) (mol/mol)	$k \times 10^3$ (L/mol min)	$k_S \times 10^3$ (L g m^2/mol min)
0.125 M MM^R	5.4	1163	4.2	5.3	37.7	0.39
0.25 M MM^R	8.2	1162	4.1	5.5	41.2 (46.2)[c]	0.39
0.50 M MM^R	14.8	1162	3.9	5.7	45.9	0.41
1.0 M MM^R	18.7	1162	2.8	5.0	54.2	–
3.0 M MM^R	18.2	1162	2.5	4.7	54.2	–
0.125 M MM^K	2.3	1164	2.7	4.3	10.3	0.15
0.25 M MM^K	10.5	1163	2.5	4.0	15.6	0.21
0.50 M MM^K	14.7	1161	2.0	4.5	19.7	0.28

[a] BAS – amount of Brønsted acid sites.
[b] PA – strength of Brønsted acid sites.
[c] 0.25 M MM^R was calcinated at 200 °C for 2 h.

the catalytic efficiency of MM^R and MM^K depends on the nature of the clay.

The nature of clay also affects the selectivity of the reaction. Thus, the increasing amount of BAS leads to the decrease in (**III**)/(**IV**) molar ratio (Fig. 6). However, the molar ratio of (**III**)/(**IV**) in the presence of acid-activated MM^R (3.9–4.2) is higher in comparison to MM^K (2.0–2.7). Moreover, the reaction rate and selectivity towards (**IIIa**–**b**) were lower in the presence of MM^K samples in comparison to MM^R (Fig. 5). Noteworthy, in the presence of MM^R and MM^K the (**IIIa**)/(**IIIb**) molar ratios were 5.3–5.7 and 4.0–4.5, respectively, that can be also related to the differences in the structural parameters. Reaction rate and isomer selectivity in the presence of MM^K with

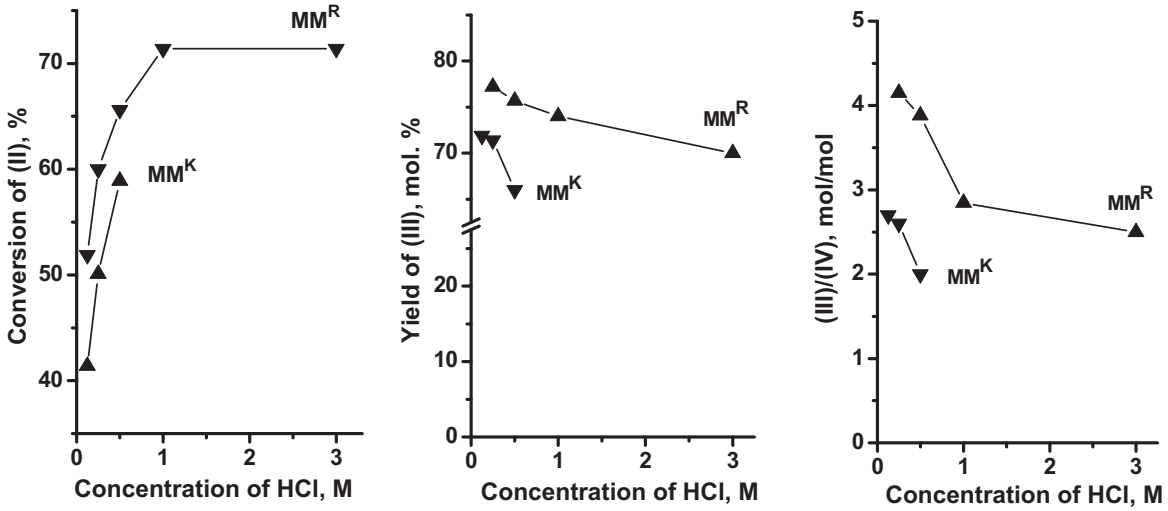

Fig. 4. Effect of HCl concentration in the conversion of (**II**), the yield of (**III**) based on consumption of (**II**) and the molar ratio of (**III**)/(**IV**), for both series of acid-activated montmorillonites, in the reaction of vanillin with (−)-isopulegol (reaction conditions: 100 mg catalyst, 0.65 mmol (**I**), 0.65 mmol (**II**) in toluene 4 mL, 35 °C, 2 h).

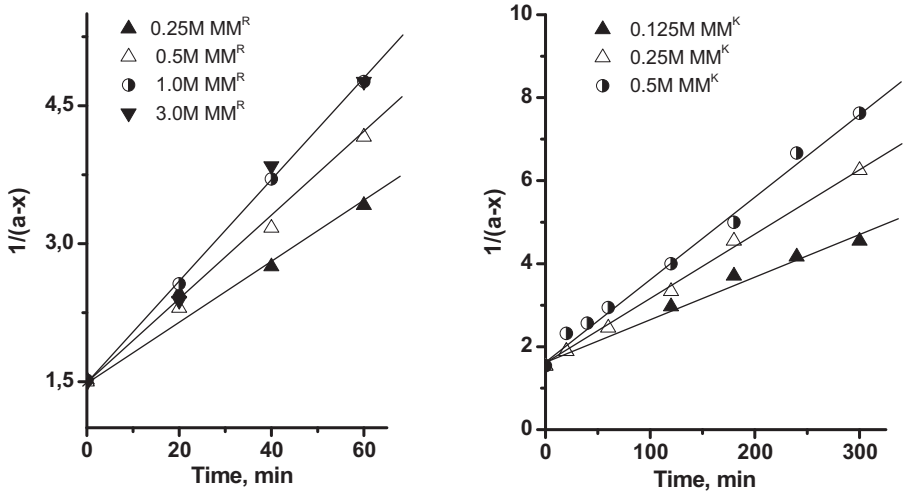

Fig. 5. Second order plots (Eq. (5)) for the synthesis of octahydro-2*H*-chromen-4-ol from vanillin and (−)-isopulegol over MM^R and MM^K catalysts (experimental conditions: 100 mg catalyst, 0.65 mmol (**I**), 0.65 mmol (**II**) in toluene 4 mL, 35 °C).

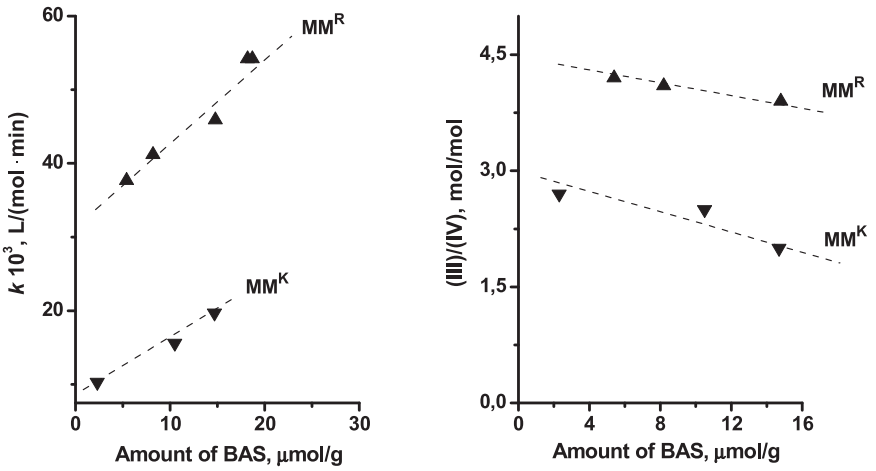

Fig. 6. Effect of the amount of Brønsted acid sites on the reaction rate and the (**III**)/(**IV**) molar ratio in the synthesis of octahydro-2*H*-chromen-4-ol from vanillin and (−)-isopulegol over MM^R and MM^K catalysts.

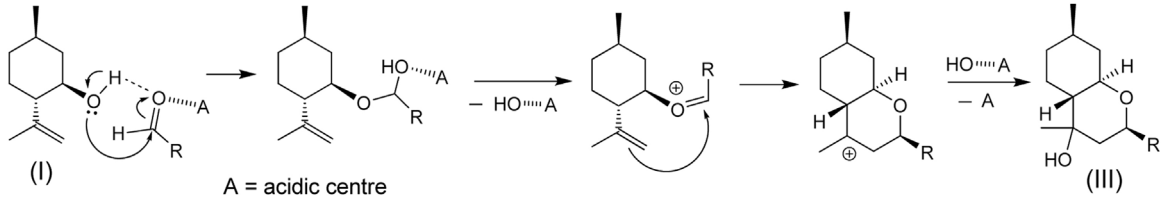

Scheme 1. Reaction mechanism proposed for the formation of (**III**).

large pore diameter and low microporosity were lower in comparison to the results found for MM^R. Taking into account the possible mechanism of formation of compound (**IIIa**–**b**) (Scheme 1), it can be proposed that the textural properties (the size and shape of the pores) can affect the accessibility of the reactants to the active sites and the spatial arrangement and configuration of the carbocation, and thereby determine the stereochemical result of the interaction. Therefore, we may conclude that the surface acidity and textural properties are crucial for catalytic activity and selectivity of acid-activated clays.

4. Conclusions

Acid-activated clays have been prepared from two calcium-rich natural layered aluminosilicates (90–95 wt.% montmorillonite) from beds located in Mukhortala (Buryatia, Russia) and Tagansk (Kazakhstan) by modification with 0.125–3.0 M HCl. Structural and textural properties were characterized by X-ray diffraction, elemental analysis and N_2-adsorption/desorption analyses. It was demonstrated that textural properties and chemical composition of acid-activated montmorillonites depend on the HCl concentration. According to IR spectroscopy using pyridine as probe molecule, the amount of BAS in the montmorillonites rises with increasing HCl concentration, while the strength of Brønsted acid sites varied negligibly.

The acid-activated montmorillonites were tested in the Prins cyclization reaction of (−)-isopulegol with vanillin to octahydro-2*H*-chromen-4-ol in toluene. It was found that the amount of BAS in acid-activated montmorillonites is a key factor for the adjustment of the reaction rate and the selectivity of the reaction. An increase of the amount of BAS leads to a decrease in the related (**III**)/(**IV**) products. The nature of the clay affects the catalytic activity and isomer selectivity, i.e. molar ratios of (**III**)/(**IV**) and (**IIIa**)/(**IIIb**). Reaction rate and isomer selectivity in the presence of MM^K with large pore diameter and low microporosity were lower in comparison to MM^R.

Acknowledgments

This work was supported by RFBR (Grants 14-03-00854 and 14-05-00297), SB RAS project V.44.2.12 and the Ministry of Education and Science of the Russian Federation. AG and MAV thank the support from the Spanish Ministry of Economy and Competitiveness (*MINECO*) and the European Regional Development Fund (*FEDER*) (project MAT2013-47811-C2-R).

References

[1] O.S. Mikhalchenko, K.P. Volcho, N.F. Salakhutdinov, in: L. Torrioni, E. Pescasseroli (Eds.), New Developments in Aldehydes Research, Nova Science Publishers, New York, 2013, pp. 49–80.
[2] N.M. Nasir, K. Ermanis, P.A. Clarke, Org. Biomol. Chem. 12 (2014) 3323–3335.
[3] I.V. Il'ina, K.P. Volcho, O.S. Mikhalchenko, D.V. Korchagina, N.F. Salakhutdinov, Helv. Chim. Acta 94 (2011) 502–513.
[4] G. Baishya, B. Sarmah, N. Hazarika, Synlett 24 (2013) 1137–1141.
[5] M. Breugst, R. Gree, K.N. Houk, J. Org. Chem. 78 (2013) 9892–9897.
[6] R. Pal, T. Sarkar, S. Khasnobis, Arkivoc 1 (2012) 570–609.
[7] A. Macedo, E.P. Wendler, A.A. Dos Santos, J. Zukerman-Schpector, E.R.T. Tiekink, J. Braz. Chem. Soc. 21 (2010) 1563–1571.
[8] J.S. Yadav, B.V. Subba Reddy, A.V. Ganesh, G.G.K.S. Narayana Kumar, Tetrahedron Lett. 51 (2010) 2963–2966.
[9] K. Zheng, X. Liu, S. Qin, M. Xie, L. Lin, C. Hu, X. Feng, J. Am. Chem. Soc. 134 (2012) 7564–17573.
[10] L.F. Silva Jr., S.A. Quintiliano, Tetrahedron Lett. 50 (2009) 2256–2260.
[11] M.K. Yadav, C.D. Chudasama, R.V. Jasra, J. Mol. Catal. A 216 (2004) 51–59.
[12] M.P. Hart, D.R. Brown, J. Mol. Catal. A 212 (2004) 315–321.
[13] C.N. Rhodes, M. Franks, G.M.B. Parkes, D.R. Brown, J. Chem. Soc. Chem. Commun. (1991) 804–807.
[14] R.V. Jasra, Bull. Catal. Soc. India 2 (2003) 157–183.
[15] A.A. Davydov, Molecular Spectroscopy of Oxide Catalyst Surfaces, John Wiley, England, 2003.
[16] B.Y. Lynne, K.A. Campbell, N. Z. J. Sediment. Res. 74 (2004) 561–579.

[17] M.G.F. Rodrigues, Cerâmica 49 (2003) 146–150.
[18] J.D. Russell, A.R. Fraser, in: M.J. Wilson (Ed.), Clay Mineralogy: Spectroscopic and Chemical Determinative Methods, Chapman & Hall, London, 1996, pp. 11–67.
[19] V.C. Farmer, in: H.V. Olphen, J.J. Fripiat (Eds.), Data Handbook for Clay Materials and Other Non-metallic Minerals, Pergamon Press, 1999, pp. 285–337.
[20] S. Bodoardo, F. Figueras, E. Garrone, J. Catal. 147 (1994) 223–230.
[21] B. Tyagi, C.D. Chudasama, R.V. Jasra, Spectrochim. Acta A 64 (2006) 273–278.
[22] H.O. Pastore, S. Coluccia, L. Marchese, Ann. Rev. Mater. Res. 35 (2005) 351–395.
[23] M. Vlasova, G. Dominguez-Patino, N. Kakazey, M. Dominguez-Patino, D. Juarez-Romero, Y. Enriquez-Mendez, Sci. Sinter. 35 (2003) 155–166.
[24] S. Guggenheim, A.F. Koster van Groos, Clays Clay Miner. 49 (2001) 433–443.